

Inspection of Shiny Surface using a Laser Range Finder

IL DONG YUN*, JA SEONG KU and SANG UK LEE †
School of Electrical Engineering, Seoul National University

Abstract

Since the surface reflectance is a function of the geometrical components and the physical surface characteristics, the reflectance parameters can be estimated from the brightness, range data and its relation, *i.e.* reflectance function. In this paper, we estimate the surface reflectance parameters by applying the partially linear method to the simplified Torrance-Sparrow reflectance model and inspect the flaws on shiny surfaces by using the estimated reflectance parameters. In order to extend the dynamic range of CCD of laser finder, we also introduce the pseudo brightness, instead of the brightness. The proposed algorithm is tested on the synthesized and real output of a laser range finder.

1 Introduction

One of the primary goals of machine vision is to recover physical properties of a scene from images. For such purpose, many researchers have investigated various reflectance models and complicate imaging process [2, 6, 7]. For instance, since the surface reflectance is directly related to surface polish and roughness, it is an important inspection criteria in many industrial applications, such as inspecting surface deformations in silicon wafers or detecting flaws in the painted exterior of cars [4, 5].

The reflectance property of a surface can be described in terms of two features: a geometric term describing the relationship between the surface orientation and light reflection, and a physical term describing the intrinsic properties of object surface. However, it is well known that the employment of only the brightness information leads to an ill-posed problem [1], and none of the intensity only based algorithms are capable of modeling the specular highlights successfully.

In order to examine the reflectance properties, the understanding of the reflectance mechanism is essential. The Torrance-Sparrow (TS) illumination

model [2] has been generally considered in both computer graphics and computer vision areas as a good physics-based model to describe the specular reflection of rough surfaces. However, since this model is complicated in nature, the simplified TS (STS) model has been widely used instead [4, 5].

Fortunately, several reflectance parameter estimation algorithms for the STS model such as partial linear method (PLM) [5] can prove the sufficiency of the input. Thus, we estimate the surface roughness based on the STS model using the PLM.

Among the various range finders, in this paper, the laser range finder is used, since the laser range finder provides several advantages over the conventional image-based range finders. The main advantage is that the laser range finder is independent to ambient light because it employs an optical filter to pass only the laser light. Therefore, although the reflectance is generally a function of wavelength of incident light, we don't need to consider the spectral context of reflectance in the proposed estimation algorithm. However, since the structure of laser camera is different from the conventional CCD camera, we present the image formation model of the laser range finder in Section 2.

2 Reflectance and Image Formation Models

In general, the image intensity depends on the light flux or light energy received by the surface, the amount of light reflected by the surface in the direction of the viewer, and the surface type. Thus, the BRDF (bidirectional reflectance distribution function) has been introduced to describe the light reflection characteristic.

2.1 Torrance-Sparrow Model

Experimentally the physicists have observed how the light is reflected from rough surfaces, and have attempted to develop the physical models to account for their observations. Torrance and Sparrow[2] developed a technique that models the surfaces as a collection of microfacets oriented in random directions. However, for the sake of simplicity, the effects

*Address: Video Research Center, Team 2, DAE-WOO Elec., Seoul, 100-741, Korea. E-mail address : yun@phoenix.dwe.co.kr

†Address: School of Electrical Engineering, Seoul National University, Seoul, 151-742, Korea. E-mail address: sanguk@asrispsn1.snu.ac.kr

of geometric attenuation factor and Fresnel coefficient could be ignored under the assumption that the incident angle and viewing angle are at most 60° [4, 5]. In this case, the BRDF for the simplified Torrance-Sparrow (STS) model f_r^S is given by

$$f_r^S = w_d \frac{1}{\pi} + w_s \frac{P(\alpha, \sigma_r)}{4 \cos \theta_v \cos \theta_i}, \quad (1)$$

where $P(\alpha, \sigma_r)$ represent the micro-facet distribution and w_d and w_s are the weighting factors for diffuse and specular component, respectively.

2.2 Structure of Laser Camera

To obtain a proper image formation model, it is essential to understand the structure of laser camera. The laser camera used in this paper employs the synchronized spot scanning technique [8]. Fig. 1 shows the synchronized spot scanning geometry that employs two sides rotating mirror OM. If we have an information on the position of the image on the detector, then the (y, z) coordinates of the spot on the object can be easily calculated. The coordinate x is obtained by mounting the camera on a sliding table. While the position of the imaged spot on the CCD provides the information needed for range measurement, and the brightness can be obtained from the amplitude of the signal.

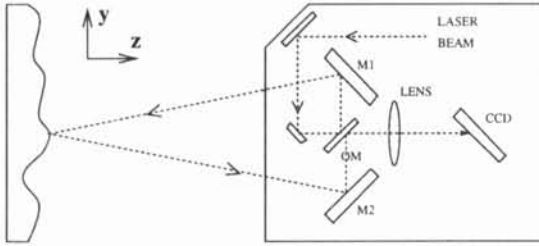


Fig. 1: The structure of laser camera

2.3 Image Formation Model

When the radiance of the point light source comes from only one direction (θ_i, ϕ_i) , we can express the scene irradiance as

$$L_i = \frac{I_0}{r^2} \cos \theta_i \frac{\delta(\theta_x - \theta_i) \delta(\phi_x - \phi_i)}{\sin \theta_i}, \quad (2)$$

where r is the distance between a light source and a measured point, and I_0 as the radiance of light source, respectively. Given a BRDF f_r and a point light source, the radiance of reflected light along the viewing direction (θ_v, ϕ_v) can be computed from

$$\begin{aligned} L_r &= \int_{\Omega_x} f_r(\mathbf{i}, \mathbf{n}, \mathbf{v}) L_i d\omega_x, \\ &= f_r \frac{I_0}{r^2} \cos \theta_i. \end{aligned} \quad (3)$$

It should be noted that L_r is inversely proportional to the square of distance r because the scanning mechanism of the laser camera is so called the synchronizing spot scanning [8].

Imaging geometry describes the relation between a surface point and its corresponding imaged point, i.e., scene radiance L_r and image irradiance E . By taking account of the *lens collection effect* [1], the relation between the image irradiance E and the scene radiance L_r is given by

$$E = \frac{\pi}{4} \left(\frac{d}{f} \right)^2 \cos^4 \gamma L_r, \quad (4)$$

where d is the diameter of lens and γ is the angle between the ray from the object point to the center of projection and the optical axis, respectively.

Now, let us derive the image irradiance E from a given reflectance and image formation models. For a notational simplicity, we shall denote the position vector by \mathbf{x} , including all geometric information and the reflectance parameter vector $\mathbf{p} = [k_d, k_s, \sigma_r]^T$. The image irradiance E can be expressed as

$$E(\mathbf{x}, \mathbf{p}) = \left(k_d \cos \theta_i + k_s \frac{P}{4 \cos \theta_v} \right) \frac{\cos^4 \gamma}{r^2} I_0. \quad (5)$$

3 Reflectance Parameter Estimation

In the context of the optimization techniques, the reflectance parameter estimation problem is equivalent to finding the reflectance parameter vector \mathbf{p} , which minimizes the following cost function over a homogeneous object surface \aleph :

$$\min_{\mathbf{p}} \sum_{\mathbf{x} \in \aleph} \left(I(\mathbf{x}) - E(\mathbf{x}, \mathbf{p}) \right)^2, \quad (6)$$

where $I(\mathbf{x})$ represents an observed brightness and $E(\mathbf{x}, \mathbf{p})$ is an estimated intensity at a point \mathbf{x} . Notice that (6) is a nonlinear optimization problem because of the parameter σ_r .

Kay and Caelli [5] first used the PLM to estimate the reflectance parameter. In the STS model, the cost function is linear in k_d and k_s , but nonlinear in σ_r . However, for a fixed σ_r , the optimal k_d and k_s can be obtained with the least square method. Therefore, the cost function can be minimized using any one dimensional techniques. Moreover, since the surface roughness is a bounded variable, the optimal value is easily obtained.

4 Experiments

In this section, we first perform several experiments to verify the derived image formation model. Then,

we present the experiment results with the synthesized and real data to demonstrate the performance of the reflectance parameter estimation.

First, we conduct an experiment to verify the image formation model derived in Section 2. Since, in this paper, a point light source in (2) is assumed, the image irradiance in (4) is inversely proportioned to the square of distance between the observed point and light source. To observe the effect of change in distance, the brightness is measured as the incident and viewing angles are fixed and the distance is linearly increased from 180mm to 440mm. As shown in Fig. 2, the measured image irradiance, *i.e.*, the brightness is close to the theoretical value, $\frac{d}{r^2}$, where d is a scaling constant.

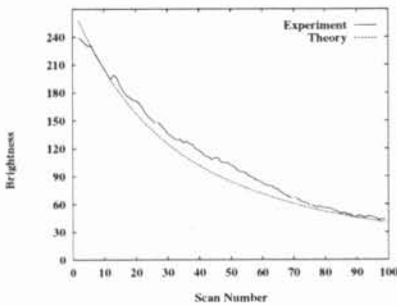


Fig. 2: The brightness change as the distance varies.

Next, let us examine the effect of the *lens collection effect* described in (4) and (5). Contrary to the previous experiment, the brightness is measured by fixing the distance to 155mm, while varying the incident and viewing angles. Moreover, to exclude the specular component in (5), we use a flat panel which slants against the laser scanning plane ($y-z$ plane). Note that the specular component is exponentially decrease as the angle α in (1) increases. As shown in Fig. 3, a close agreement between the measured brightness and the theoretical value, $c \cos \theta_i \cos^4 \gamma$, where c is also a scaling constant, is also observed.

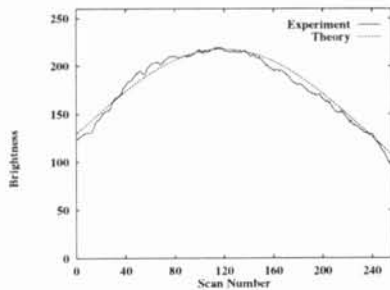


Fig. 3: The effect of lens collection effect: brightness

To show the performance of the PLM, the overall estimation error as varying the roughness is presented in Fig. 4. The minimum position can be easily identified using the golden section search [9]. The

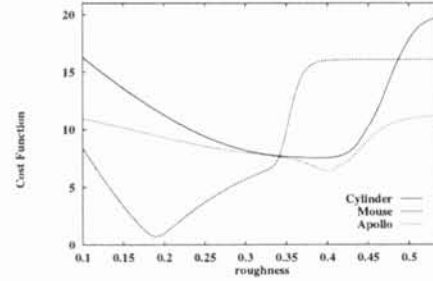


Fig. 4: The comparison of cost values as the varying surface roughness for the synthetic data (Cylinder, PC Mouse, and Apollo Statue), when the PLM is applied to the STS model.

estimated parameters at the minimum position are compared quantitatively with the true values in Table 1, which shows that the PLM is sufficient to our purpose.

Table 1: Parameter estimation performance of Partial Linear Method.

	Apollo	Mouse
Parm.	(k_d, k_s, σ_r)	(k_d, k_s, σ_r)
True	(1.000 1.500 0.400)	(0.320 0.400 0.190)
Est.	(0.993 1.454 0.401)	(0.318 0.397 0.189)

The proposed reflectance parameter estimation algorithm is also tested on the real range and brightness data. Fig. 5 shows the measured brightness data, and the estimated brightness data for Apollo statue. The estimated reflectance parameters (k_d, k_s, σ_r) are (0.623 1.327 0.407).

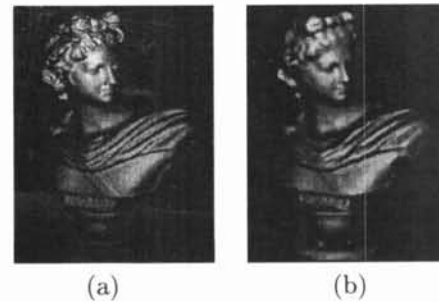


Fig. 5: Experiment on Apollo statue: (a) measured brightness data (b) estimated brightness data

Fig. 6 also shows the measured and estimated brightness data for the PC mouse. Note that the estimated roughness is 0.183 rad, which is more smooth than the Apollo statue. Therefore, the proposed algorithm can be applied to discriminate two similarly looking objects with different roughness. Notice that it is very difficult task for brightness data only used approaches.

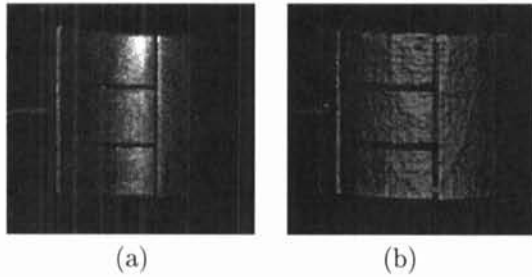


Fig. 6: Experiment on computer mouse: (a) measured brightness data and (b) estimated brightness data

5 Detecting Flaws on Shiny Surface

One of the difficulties in measuring the brightness data is that the ratio of specular to diffuse reflection for shiny surface exceeds the dynamic range of CCD [7]. By controlling the shutter speed of camera, Wolff could raise the ratio of specular to diffuse reflection up to about 3000:1. The laser camera can not adjust the shutter speed or iris, but instead can control the laser power pointwise. We can extend the limit of dynamic range using the differentiation of E against the radiance of light source I_0 . From (5), we can easily obtain the $\partial E/\partial I_0$, which is referred to as a *pseudo brightness*. To see the validity of the pseudo brightness, a test is performed on 3 different points in cylinder-shaped plaster as shown in Fig. 7 (a). The brightness as varying the laser power on these points linearly is presented in Fig. 7 (b). The slopes of each point A, B, C are 27.5, 24.2, and 16.7, respectively. One can find that the slopes are nearly constant in the middle range of brightness. The steeper slope in the Fig. 7 (b) corresponds to the brighter point in the Fig. 7 (a). Whereas, the brightness of these points are 220, 191, and 132, respectively. Note that the ratio of the pseudo brightness are very close to those of brightness, implying that the pseudo brightness can substitute for the brightness.

Now, let us explain how to acquire the pseudo brightness image. First, a proper range of laser power should be searched on each point. When the laser power is set to the proper value, the measured brightness would be in [40, 230]. Then, we can calculate the average change of the brightness against the laser power increasing. As an example, the proper ranges of laser power and its center power for a shiny object are shown in Fig. 8 (a). The measured brightness for fixed power, and the obtained pseudo brightness is presented in Fig. 8 (b). Note that there are background points over the 233th point in Fig. 8 (b). One can easily find that the brightness can not properly be measured for any fixed power. More specifically, the brightness is saturated or not measured when the

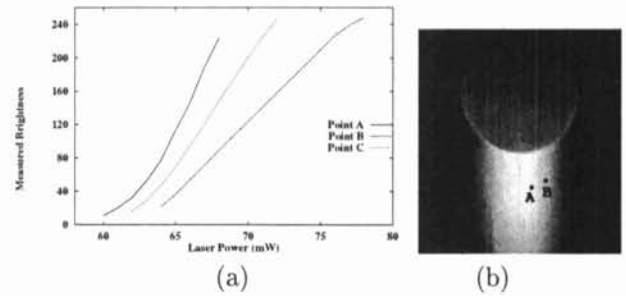


Fig. 7: An example to explain the notion of the pseudo brightness: (a) Measured brightness for a fixed point as varying laser power. The slopes of each point A, B, C are 27.5, 24.2, and 16.7, respectively. (b) The measured brightness image of cylinder shaped plaster and three corresponding points A, B, C. The brightness of these points are 220, 191, and 132.

laser powers are set to 80mW and 67mW, respectively. However, when the laser power is set to the center power pointwisely, the measured brightness is always in a range of [80, 140], except for background points.

The exterior of car is normally heated to polish its surface after spraying paint. The defect in heat treating process is nearly impossible to detect by the conventional image-based vision system, since the difference between the normal and the defected is caused by its color and surface roughness. Fig. 9 (d) shows the inspection object, *i.e.*, a car bumper.

Fig. 9 shows also the results of experiment: the measured brightness, the estimated brightness, and the candidates of defect where the absolute difference between the measured and estimated brightness is larger than a threshold. By considering the noise level of the laser camera, the threshold is set to 15 empirically. From the result shown in Fig. 9 (c), there are three different types of defect, denoted by *type I*, *II* and *III* errors, respectively. The *type I* error is mainly due to the range data itself, since the range finder can not acquire a range data properly in the edge or in the narrow wedge of the object (see the black regions in Fig. 9 (b)). The *type III* error is caused by specular spike component on which the surface behaves like a mirror. Since this component is not considered in (5), the brightness could not be accurately estimated for the specular spike. Fortunately, the *type I* and *III* can be eliminated from the range information. Therefore, we can only detect the *type II*, mainly caused by the difference of surface roughness and/or color.

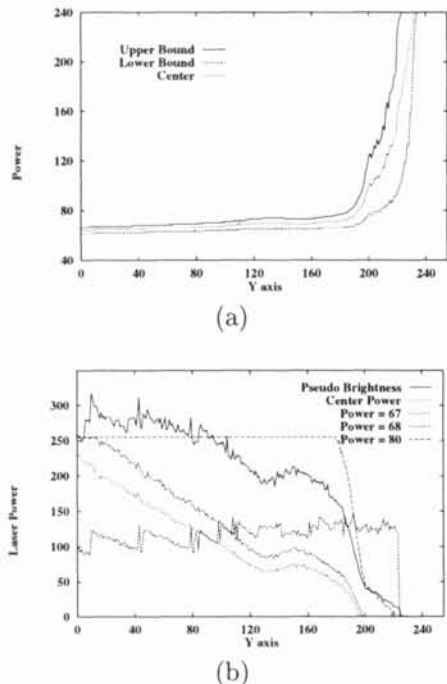


Fig. 8: An example to explain how to acquire the pseudo brightness: (a) proper scopes of laser power and its center power, (b) The 3 measured brightness for fixed power 67, 68, 80, one measured brightness for center laser power of the proper scope, and the calculated pseudo brightness

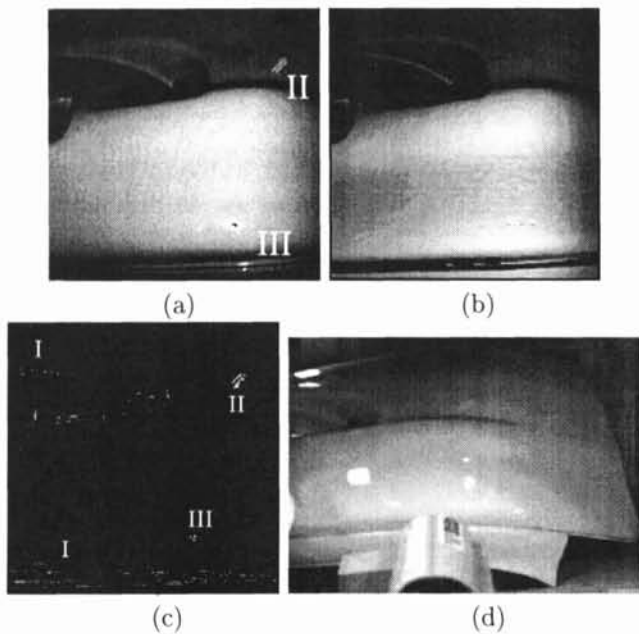


Fig. 9: An inspection on a bumper: (a) the brightness captured by the laser camera, (b) the estimated brightness from the range and reflectance parameters, and (c) the difference image between (a) and (b), (d) the brightness captured by a TV camera. estimation error.

6 Conclusion

In this paper, we have estimated the reflectance parameters based on the range and brightness data of a laser range finder which is robust against the environmental condition. The structure of laser camera and lens collection effect have been considered, and a proper image formation model was derived for the laser camera. The proposed algorithm employs the simplified Torrance Sparrow Model. As an application, the estimated reflectance parameters were applied to inspect the surface defects on homogeneous material, which may have different shape or position. For this application, we also introduced the pseudo brightness to extend the dynamic range of CCD sensor of the laser camera.

References

- [1] B. K. P. Horn, *Robot Vision*, MIT Press, 1986.
- [2] K. E. Torrance and E. M. Sparrow, "Theory for off-specular reflection from roughened surfaces," *Journal of Optical Society of America*, vol. 57, no. 9, pp. 1105-1114, Sep. 1967.
- [3] G. Healey and T. O. Binford, "Local Shape From Specularity," *Proceedings of IEEE International Conference on Computer Vision*, pp. 151-160, London, June 1987.
- [4] K. Ikeuchi and K. Sato, "Determining Reflectance Properties of an Object Using Range and Brightness Images," *IEEE Trans. Pattern Analysis and Machine Intelligence*, vol. 13, no. 11, pp. 1139 - 1153, Nov. 1991.
- [5] G. Kay and T. Caelli, "Inverting an Illumination Model from Range and Intensity Maps," *CVGIP: Image Understanding*, vol. 59, no. 2, pp. 183 - 201, Mar. 1994
- [6] S. K. Nayar, K. Ikeuchi, and T. Kanade, "Surface Reflection: Physical and Geometrical Perspectives," *IEEE Trans. Pattern Analysis and Machine Intelligence*, vol. 13, no. 7, pp. 611-634, July 1991.
- [7] L. B. Wolff, "Relative brightness of specular and diffuse reflection." *Optical Engineering*, vol. 33, no. 1, pp. 285-293, Jan. 1994.
- [8] *SCAN-3000 USER'S GUIDE*, SERVO ROBOT Inc., 1993.
- [9] W. H. Press, B. P. Flannery, S. A. Teukolsky and W. T. Vetterling, *Numerical Recipes in C: The Art of Scientific Computing*, Cambridge University Press, Cambridge, 1988.